GBT S-band (2 GHz): Pointing

Dana S. Balser, Ronald J. Maddalena, Frank Ghigo, & Glen I. Langston

23 March 2001

Abstract

All sky pointing observations at S-band are discussed. A traditional pointing model including eight physical terms are used to fit the data. The all sky rms is $8\farcs5$.

1 Introduction

The philosophy has been to first determine the focus tracking model empirically using astronomical observations, supported by metrology measurements, and then to turn focus tracking on for the all sky pointing observations. Currently, the focus tracking model has been determined in the X and Y directions only. The sub-reflector can only move ~ 1.5 inches in Z and thus there is not enough range to detect significant changes in the gain. The focus tracking observations and analyses are discussed in another report.

The first all sky pointing observations have been made with the GBT at S-band (2 GHz). These observations are discussed in §2. The results are given in §3. A preliminary analysis of the data was made using AIPS++. The data were then imported into the program TPOINT for further analysis. The conclusions are in §4.

2 Observations

Observations were made during two epochs: 2001 March 09–10 (project = pnt_lowgreg_09) and 2001 March 12–13 (project = pnt_lowgreg_10). All pointing sources were selected from the NVSS pointing calibrator list (Condon & Yin 2001). At 2 GHz the GBT half-power beam-width (HPBW) is $6'$. The catalog lists the maximum beam size ($\theta_{\rm m}$) where the calibrator source is unconfused. Therefore, sources were selected with $\theta_{\rm m} \geq 360''$. Also, only sources brighter than 2 Jy at 2 GHz were selected. Here we assume that $F_\nu \propto \nu^{-0.7}$.

The all sky pointing observations were scheduled using the CLEO application *scheduler*. This is an interactive program which loads in a pointing catalog, computes slew and observing times, allows the user to select pointing objects interactively, and then writes out a GO observing table. Slew rates were estimated to be $15\fdg8$ per minute in azimuth with an

acceleration time of 0.2 minutes, and 7.°8 per minute in elevation with an acceleration time of 0.09 minutes. A procedure time of 2.75 min was initially estimated. This included the time to perform the crosses, fill and analyze the data, and update the local pointing corrections (LPCs). Depending on how quickly the operator responded this time was typically 3.25–4.00 min. Therefore a couple of pointing sources in the GO table were skipped every hour.

The GO procedure *peak* was used to determine LPCs. The procedure *peak* performs two raster scans in RA ($W \rightarrow E$ and then $E \rightarrow W$). The procedure then pauses. An event is sent to an AIPS++ client which fills the data using *gbtmsfiller*, and then calculates the LPCs. If acceptable the LPCs are updated automatically and then the procedure performs two raster scans in Dec ($S \rightarrow N$ and then $N \rightarrow S$). Again the data are filled, analyzed, and the LPCs updated pending user verification. A telescope rate of $90'$ per minute was used with a length of $45'$ and an integration time of 0.5 s. Typically, the source was easily detected and reasonable LPCs computed.

Focus tracking in the X and Y directions were employed during these pointing observations. The following functions were used and determined empirically:

$$X = 9.122 - 12.589\,Cos(\mathrm{El}) - 2.529\,Sin(\mathrm{El}) \ \text{inches} \tag{1}$$

and

$$Y = -6.663 + 8.046\,Cos(\mathrm{El}) + 1.258\,Sin(\mathrm{El}) \ \text{inches} \tag{2}$$

where X and Y are the Gregorian focus directions in inches and El is the elevation. The Z focus direction was held constant with a value of zero. These observations and results are discussed in more detail in a separate report.

Several problems did occur during these all sky pointing runs. Because the M&C parameters to change the optics are defined as offsets when focus tracking is turned on, any updates to the antenna will reset the focus tracking parameters. Therefore on several occasions the focus tracking was accidently changed. The antenna manager died on at least two occasions for unknown reasons. Also after ~ 10 hr the connection between GO and the AIPS++ client would hang. This may be the result of a memory leak and is being investigated. About half of the data were deleted from pnt_lowgreg_09, while only a few scans were deleted from pnt_lowgreg_10.

3 Results

The all sky pointing runs are summarized in Figures 1–2. There are 108 and 92 points corresponding to pnt_lowgreg_09 (Figure 1) and pnt_lowgreg_10 (Figure 2), respectively. Because there were not many points at both low and high elevations for the first observing session these regions were more heavily sampled during the second observing session. Nevertheless, the distribution of points is reasonable on both days. About two-thirds of

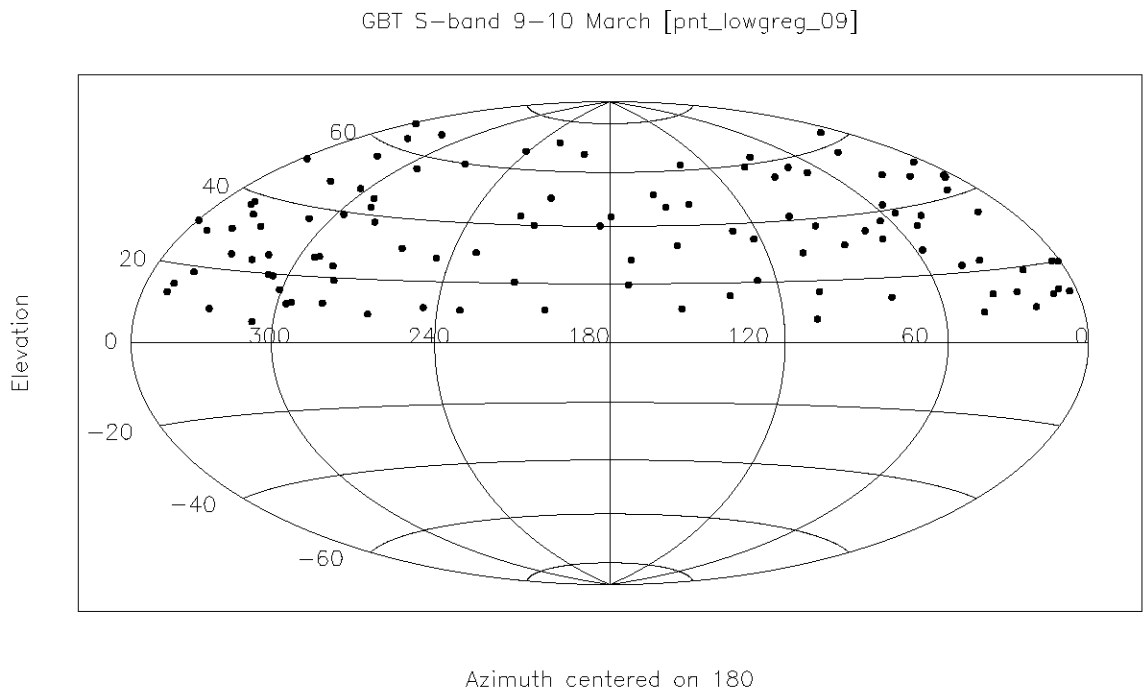

Figure 1: Distribution of sources on the sky with an aitoff projection for project pnt_lowgreg_09.

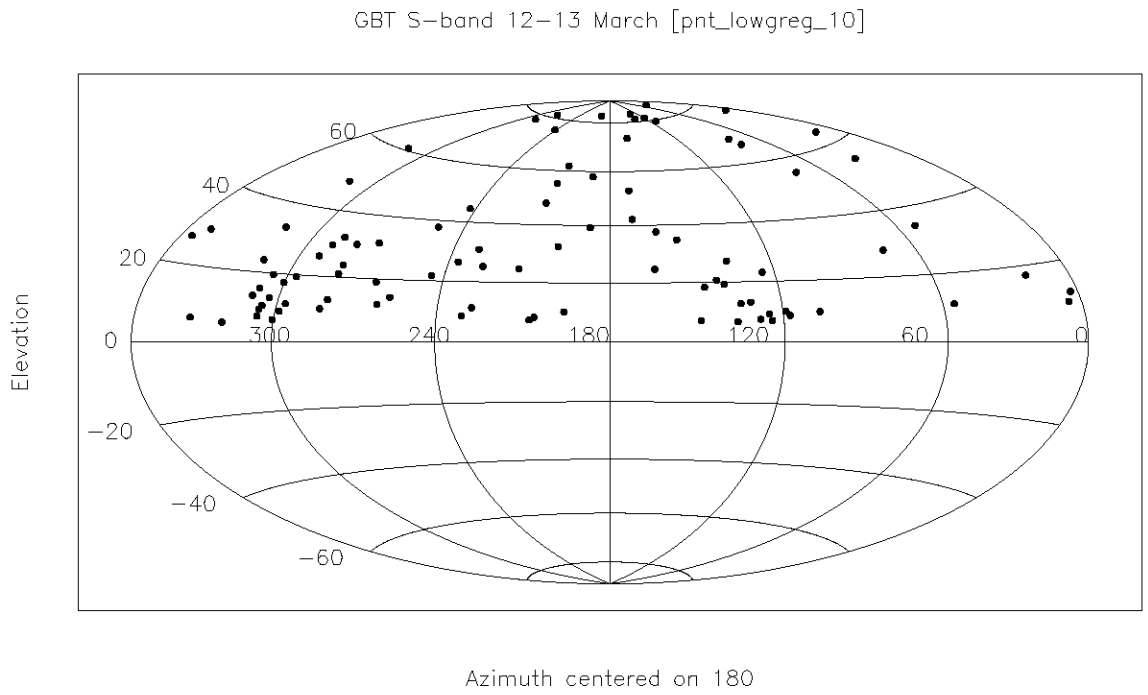

Figure 2: Distribution of sources on the sky with an aitoff projection for project pnt_lowgreg_10.

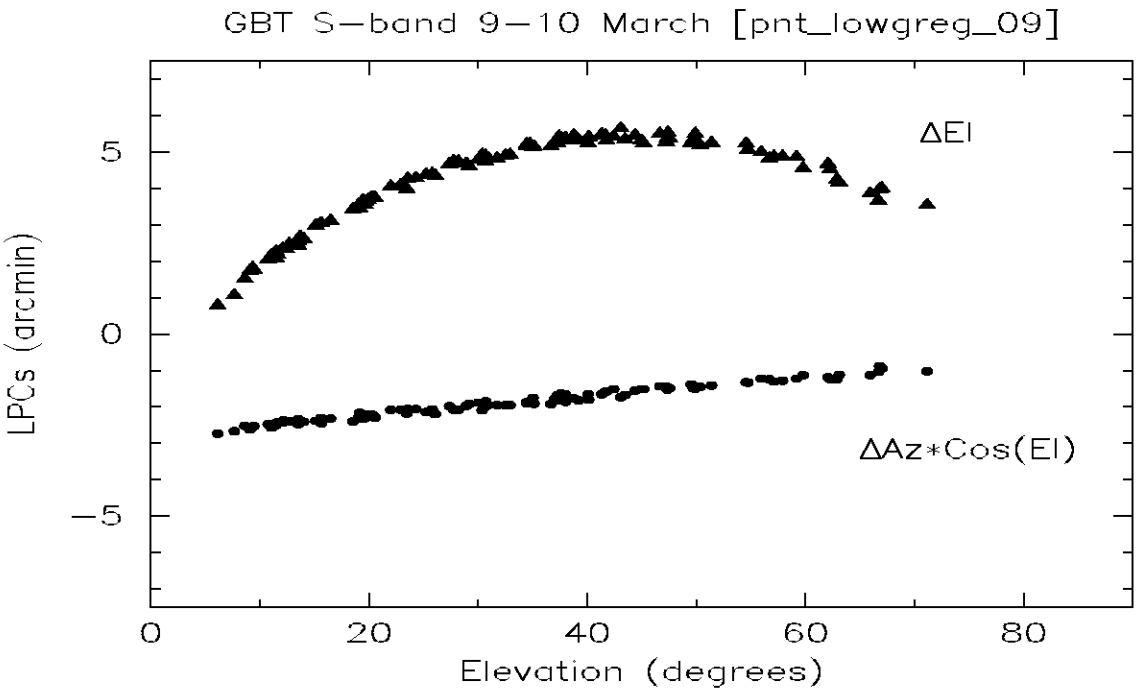

Figure 3: Local pointing corrections (LPCs) plotted as a function of elevation for pnt_lowgreg_09.

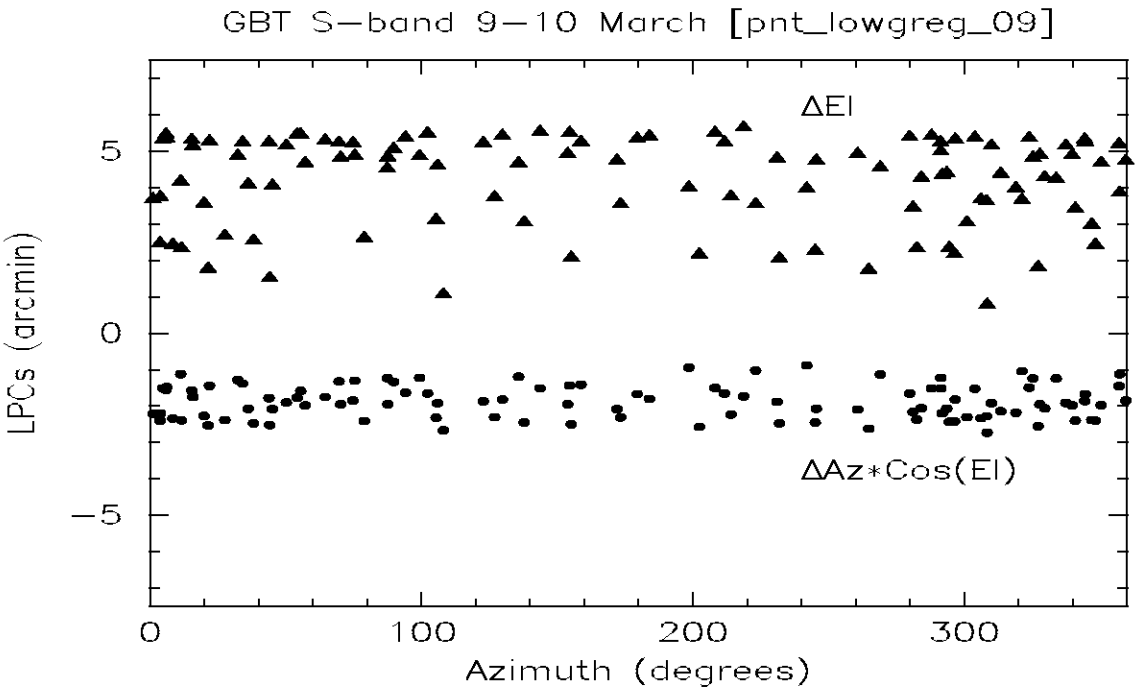

Figure 4: Local pointing corrections (LPCs) plotted as a function of azimuth for pnt_lowgreg_09.

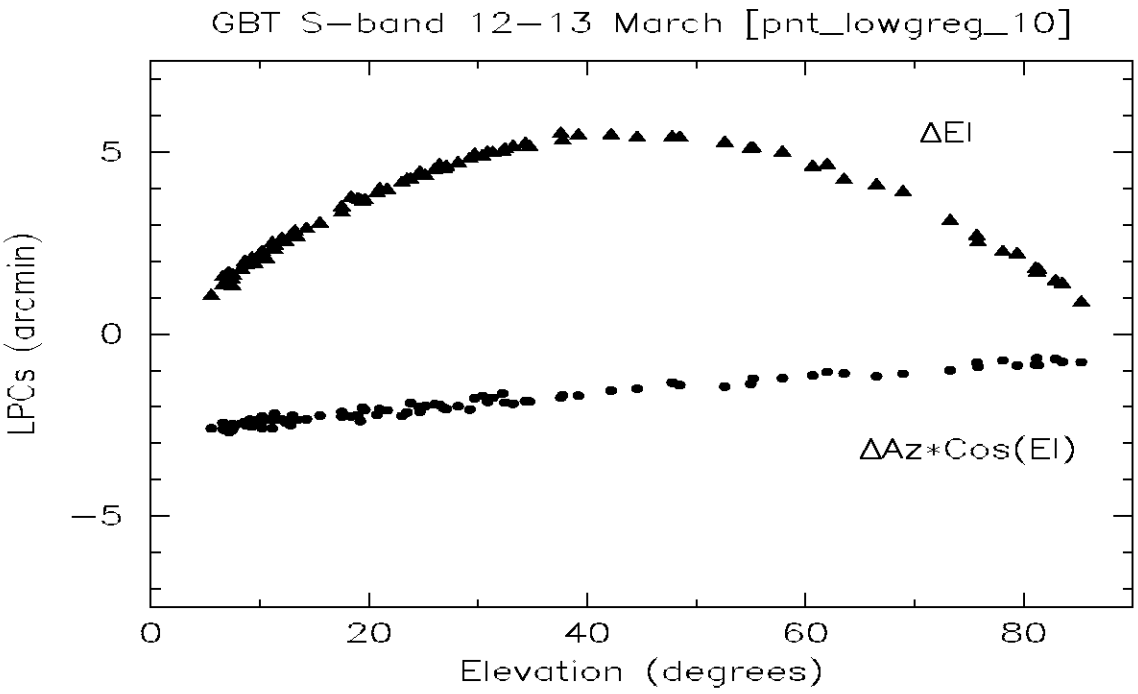

Figure 5: Local pointing corrections (LPCs) plotted as a function of elevation for pnt_lowgreg_10.

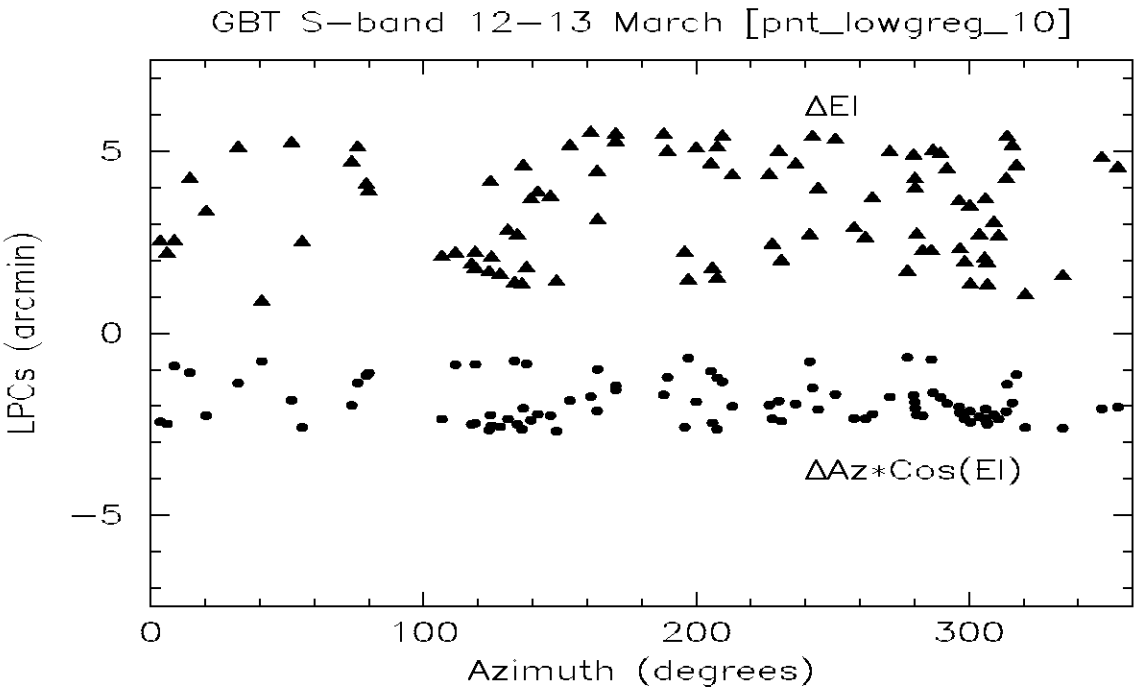

Figure 6: Local pointing corrections (LPCs) plotted as a function of azimuth for pnt_lowgreg_10.

Table 1: Azimuth Pointing Terms (ΔA Cos E)

Coeff. (M&C)	Coeff. (TPOINT)	Term	Value (arcsec)	σ (arcsec)	Meaning
$d_{0,0}$	–CA	1	+121.46	8.638	Horizontal Collimation
$b_{0,1}$	–NPAE	Sin E	–83.13	6.083	El Axle Collimation
$d_{0,1}$	–IA	Cos E	+42.53	7.187	Az Zero
$b_{1,1}$	AW	Cos A Sin E	–0.23	0.748	Zenith E-Tilt
$a_{1,1}$	AN	Sin A Sin E	–3.89	0.756	Zenith N-Tilt

Table 2: Elevation Pointing Terms (ΔE)

Coeff. (M&C)	Coeff. (TPOINT)	Term	Value (arcsec)	σ (arcsec)	Meaning
$d_{0,0}$	IE	1	+826.33	8.610	El Zero
$c_{1,0}$	–AW	Sin A	+0.23	0.748	Zenith E-Tilt
$d_{1,0}$	AN	Cos A	–3.89	0.756	Zenith N-Tilt
$b_{0,1}$	ECES	Sin E	–812.44	6.085	Asymmetric Gravity
$d_{0,1}$	ECEC	Cos E	–821.06	7.193	Symmetric Gravity

the points in pnt_lowgreg_09 are daytime observations while essentially all of the points in pnt_lowgreg_10 were taken at night-time.

The local pointing corrections (LPCs) are summarized in Figures 3–4 for pnt_lowgreg_09 and Figures 5–6 for pnt_lowgreg_10. The ΔEl versus El curves are primarily due to gravity. It is thought that the ΔAz Cos(El) versus El is curve is mostly a focus tracking motion. That is, since the Z focus was held constant at zero any motions of the feed-arm in this direction would show up as a pointing error. Metrology measurements are roughly consistent with this picture and fit the curve reasonably well (Parker 2000). There appears to be very little structure for the LPCs as a function of azimuth which implies that the track is quite flat.

The data were then imported into the program TPOINT which performs a multi-dimensional least-squares fit (Wallace 1998). Both observing runs (pnt_lowgreg_09) and (pnt_lowgreg_10) were combined for this analysis. A traditional model which includes eight physical terms was used. The pointing coefficients are listed in Tables 1 and 2 for the azimuth and elevation series, respectively. Note how the adopted pointing coefficients, based on the two-dimension Fourier series coefficients (Condon 1992, GBT Memo 75), map to the TPOINT coefficients.[1].

[1]For TPOINT due south is zero azimuth increasing eastward, while the usual convention is due north is zero azimuth increasing eastward. Therefore, $A \rightarrow -A$, $Cos(A) \rightarrow Cos(-A) = Cos(A)$, and $Sin(A) \rightarrow Sin(-A) = -Sin(A)$.

The sky root-mean-square (*rms*) is 8.″5. Notice that the plane which defines the azimuth track is essentially level with the horizon. The coefficients corresponding to the zenith tilt terms are on the order of a few arcsec. The gravity coefficients are much larger and on the order of 800″. The finite element model (MOD95) predicts $d_{0,0} = 508''$, $b_{0,1} = -367''$, $d_{0,1} = 342''$ for the elevation series (Wells 1998, GBT Memo 173). The observed deflection due to gravity is significantly larger than predicted by this version of the FEM.

The azimuth pointing coefficients $d_{0,0}$, $b_{0,1}$, $d_{1,0}$ correspond to the horizontal collimation, the elevation axle collimation, and the azimuth zero, respectively. These coefficients are quite large but are probably due to focus tracking in the Z direction. Because the Z-direction focus tracking could not be measured by observing gain variations, only the X and Y directions were active during the pointing runs. Z was held constant at zero. Metrology measurements of the deflection of the feed-arm with changes in elevation predict the $\Delta\mathrm{Az}\,\mathrm{Cos}\,\mathrm{E}$ versus elevation curves in Figures 3 and 5 (Parker 2000). Therefore, we expect that focus tracking contributes to most of the these three terms in the azimuth series. Nonetheless, until either observations are made at higher frequencies, where the focus is more sensitive, or the laser metrology system is used the focus tracking and pointing cannot be decoupled.

The results of the TPOINT analysis are summarized in a series of figures. Figure 7 shows the residuals plotted in a scatter diagram, while Figure 8 plots the pointing residuals as error vectors. The pointing residuals horizontally on the sky and in zenith angle are shown versus azimuth in Figures 9 and 10 and versus zenith angle in Figures 11 and 12. In general the fits look reasonable. There is clearly some structure, however.

The correlations in the fit are shown below. Notice that the gravity coefficients along with El zero (ECES, ECEC, and IE) are all highly correlated. Also, the three terms used to fit the azimuth LPCs (CA, NPAE, and IA), expected to be the Z focus tracking motion, are highly correlated.

```
IE      +0.0015
NPAE    +0.9273 +0.0037
CA      -0.9887 -0.0022 -0.9666
AW      -0.0670 -0.0063 -0.0559 +0.0607
AN      +0.0446 -0.0586 +0.0230 -0.0354 -0.0735
ECEC    -0.0031 -0.9884 -0.0052 +0.0037 +0.0292 +0.0726
ECES    +0.0018 -0.9666 -0.0005 -0.0011 -0.0156 +0.0519 +0.9270

          IA      IE      NPAE    CA      AW      AN      ECEC
```

TPOINT was also used to analyze the data for each pointing run separately. The results are similar between the two runs. The *rms* for each run was slightly less ($\sim 7.''5$). It should be noted that refraction was not being calculated correctly during both observation runs. Constant weather information was being used to calculate refraction. During much of the

pnt_lowgreg_09 observing it was sunny and dry, while the pnt_lowgre_10 observations were taken in the rain; hence apparent differences in the pointing are visible in the pointing at low elevations (c.f., Figures 3 and 5).

4 Conclusion

All sky pointing observations were made during two distinct periods separated by only a couple of days. A traditional pointing model consisting of eight physical terms produces a sky *rms* of 8.″5 for both observing sessions. The residuals are slightly smaller for each observing run when analyzed separately; however, this may be a result of problems with the refraction calculation and differences in the pointing at low elevations.

The zenith tilt of the track is very small (few arcsec). The gravity terms are significantly larger than those predicted by the finite element model MOD95. The physical terms associated with the azimuth series are almost certainly related to the motion of focus tracking in the Z direction which was held fixed during these pointing runs. This is supported by metrology measurements of the feed-arm.

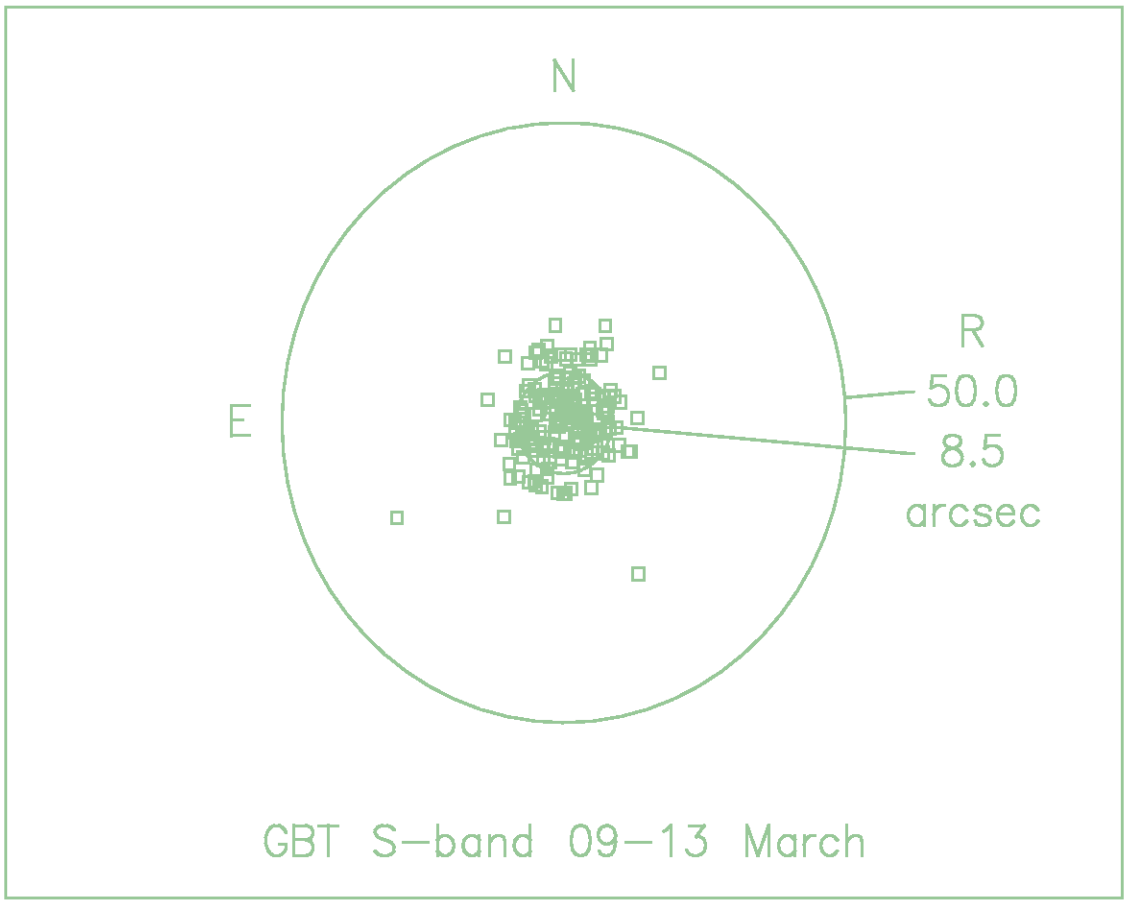

Figure 7: The residuals plotted as a scatter diagram. The inner circle is the sky *rms* of the fit (8.″5).

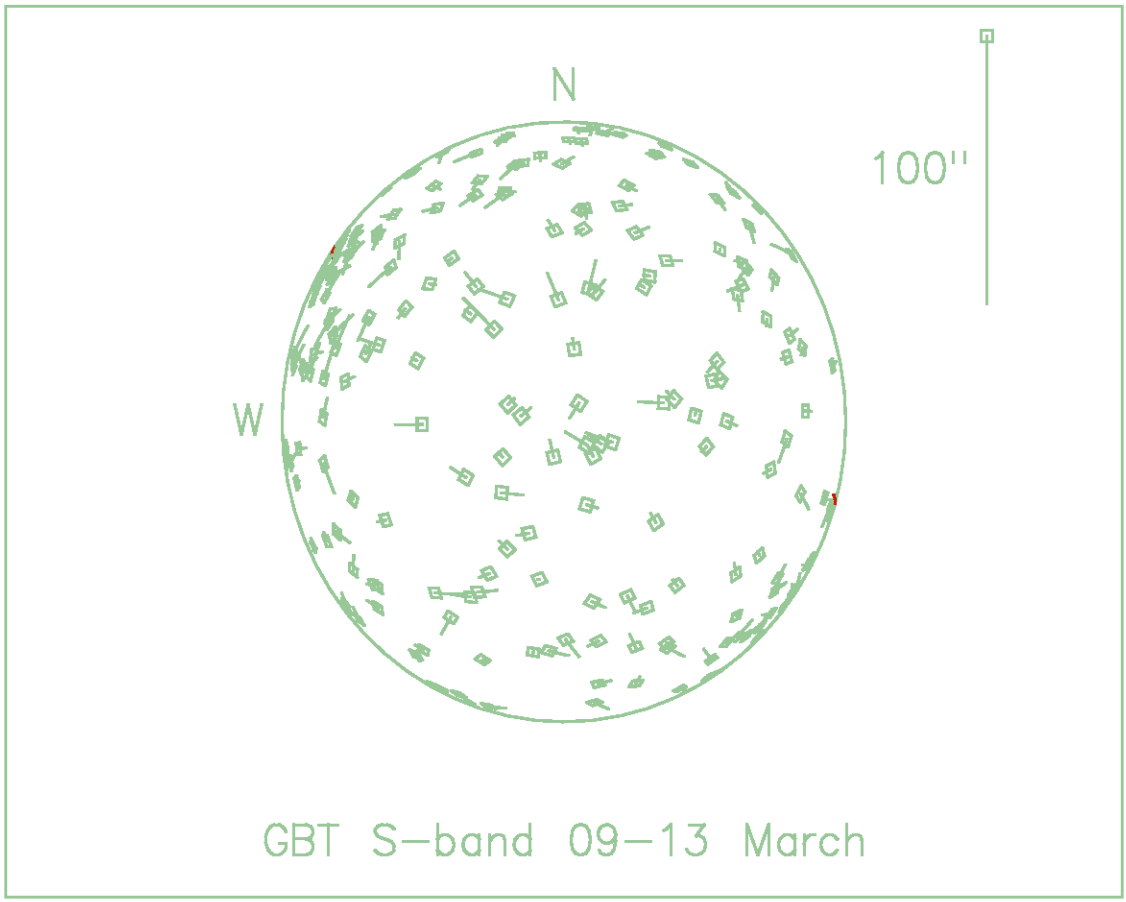

Figure 8: The pointing residuals as error vectors on an azimuthal projection.

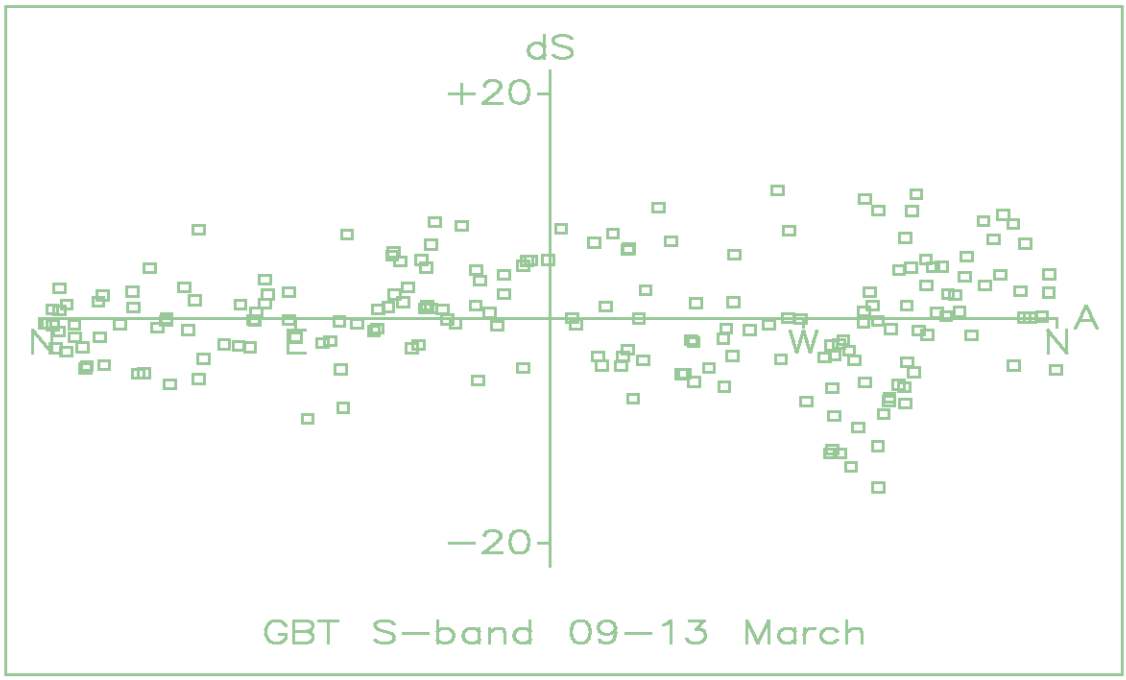

Figure 9: The pointing error horizontially on the sky (ΔA Cos E) as a function of azimuth.

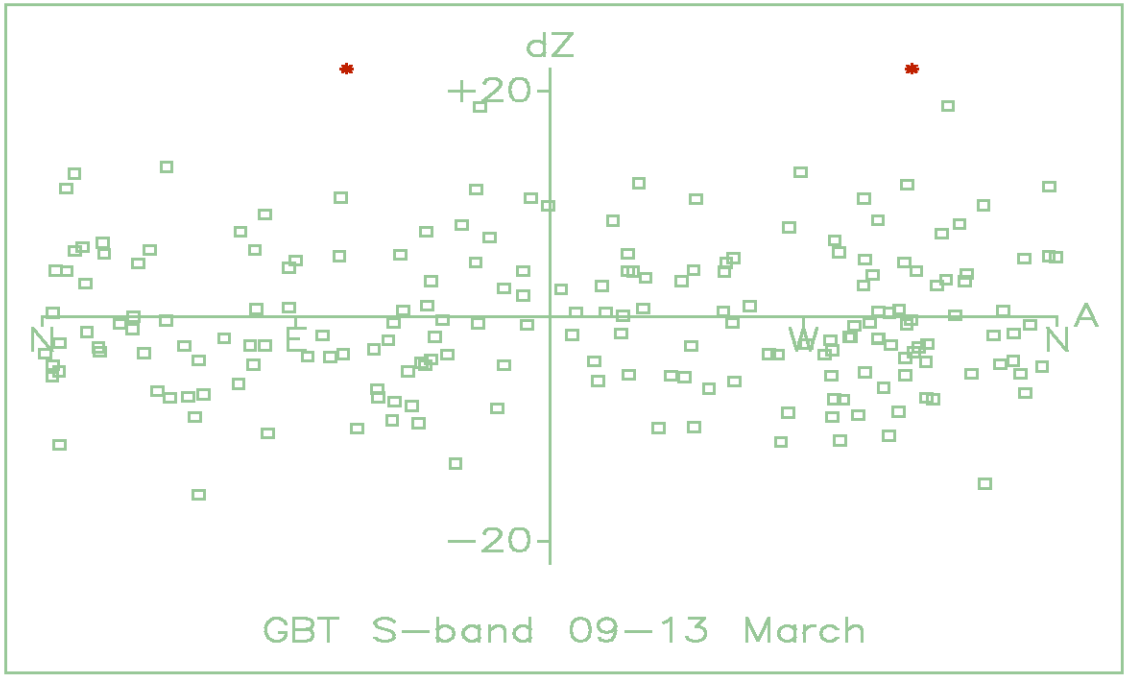

Figure 10: The pointing error in zenith angle as a function of azimuth.

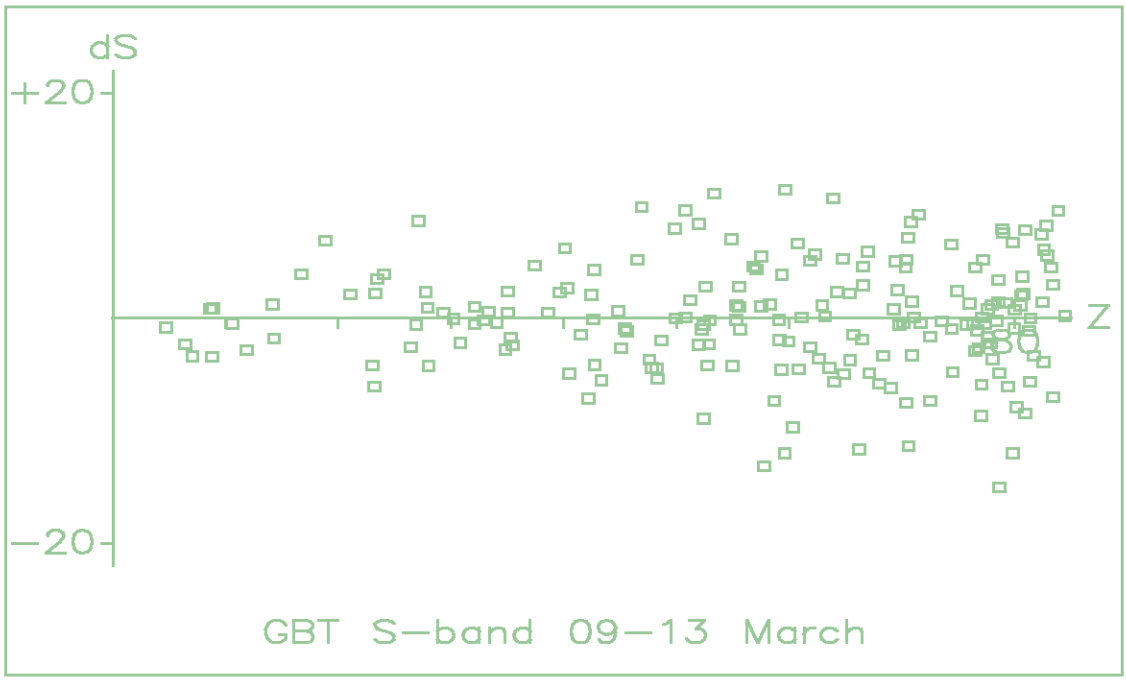

Figure 11: The pointing error horizontially on the sky (ΔA Cos E) as a function of zenith angle.

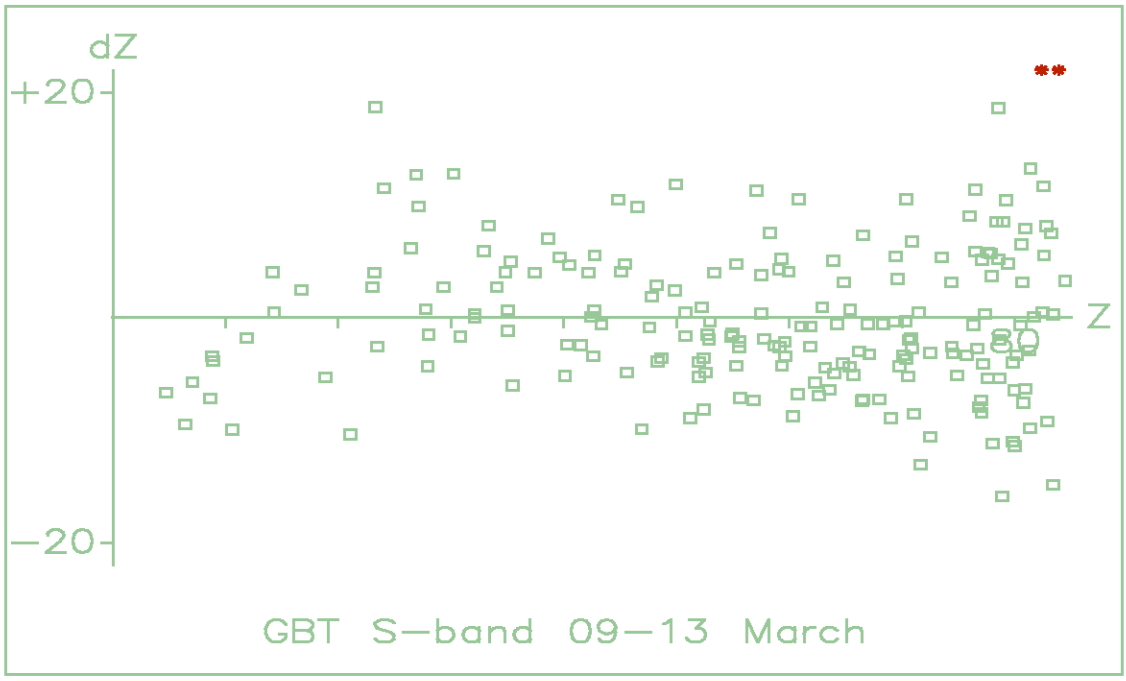

Figure 12: The pointing error in zenith angle as a function of zenith angle.